Available online at www.sciencedirect.com
SCIENCE DIRECT®
Biochimica et Biophysica Acta 1660 (2004) 118–130
BIOCHIMICA ET BIOPHYSICA ACTA
BBA
www.bba-direct.com

Molecular dynamics of the cyclic lipodepsipeptides' action on model membranes: effects of syringopeptin22A, syringomycin E, and syringotoxin studied by EPR technique

Zsófia Szabó, Marianna Budai, Katalin Blaskó, Pál Gróf*

Faculty of Medicine, Institute of Biophysics and Radiation Biology, Semmelweis University, VIII. Puskin u. 9, POB 263, Budapest H-1444, Hungary

Received 6 May 2003; received in revised form 11 November 2003; accepted 11 November 2003

Abstract

Interaction of pore-forming toxins, syringopeptin22A (SP22A), syringomycin E (SRE) and syringotoxin (ST), with model membranes were investigated. Liposomes were prepared from saturated phospholipids (DPPC or DMPC) or from binary mixtures of DPPC with varying amount of DOPC or cholesterol. The effects of the three toxins on the molecular order and dynamics of the lipids were studied using electron paramagnetic resonance (EPR) techniques. SP22A was the most-, SRE less-, and ST the least effective to increase the ordering and to decrease the rotational correlation time of the lipid molecules. The effects were more pronounced: (a) on small unilamellar vesicles (SUVs) than on multilamellar vesicles (MUVs); (b) on pure DPPC than on DPPC–cholesterol or DPPC–DOPC mixtures. Fluidity changes, determined from EPR spectra at different concentrations of the toxin, suggested the shell structure of the lipid molecules in pore formation. EPR spectra observed at different depth of the hydrocarbon chain of the lipid molecules implied an active role of the lipid molecules in the architecture of the pores created in the presence of the three toxins. Temperature dependence of the fluidity of the SUVs treated with toxins has shown an abrupt and irreversible change in the molecular dynamics of the lipid molecules at a temperature close to the pretransition, depending on the toxin species and the lipid composition. Coalescence and aggregation of the SUVs were proposed as the origin of this irreversible change.

Keywords: Cyclic lipodepsipeptide; Toxin-membrane interaction; Pore formation; Electron paramagnetic resonance; Membrane fluidity; Order parameter; Rotational correlation time

1. Introduction

Membrane-permeabilizing compounds are widespread weapons in the nature used as part of the host defense system of many species from insects to mammalians, and as toxins of pathogenic bacteria [1–11]. The structure of these peptides and lipopeptides are very different but mainly it shows an amphiphilic structure in hydrophobic environment, and possesses one or more positive charges [1,2,4,6,12–15]. The spectrum of the activity and the efficiency of these molecules depend on both the structure of the molecule and the lipid composition of the target membrane. Extensive studies on pore-forming endogenous host-defense peptides highlighted the requirement for appropriately positioned cationic residues [1,2,4]. Sitaram et al. [16,17] showed that the arrangement of charged residues was important for the activity and an increased net positive charge enhanced the antimicrobal activity in case of seminalplasmin, a 47-residue protein iso-

Abbreviations: $2A_{max}$, outer-peak separation; Chol, cholesterol; CLP, cyclic lipodepsipeptide; DLS, dynamic light scattering; DMPC, dimyristoyl-L-α-phoshatidyl-choline; DOPC, dioleoyl-phosphatidyl-choline; DOPE, dioleoyl-phosphatidyl-ethanolamine; DOPS, dioleoyl-phosphatidyl-serine; DPPC, dipalmitoyl-L-α-phoshatidyl-choline; EPR, ESR, electron paramagnetic resonance; LUV, large unilamellar vesicles; MLV, multilamellar vesicles; NLLS, nonlinear least-squares method/program; PBS, phosphate buffered saline; RBC, red blood cell; R_{prp}, perpendicular rotational diffusion coefficients; S_{20}, order parameter; SL-12, 12-doxyl-stearic acid spin label; SL-16, 16-doxyl-stearic acid spin label; SL-5, 5-doxyl-stearic acid spin label; SL-7, 7-doxyl-stearic acid spin label; SL-SPPC, 1-palmitoyl-2-stearoyl(5-doxyl)-*sn*-glycero-3-phosphocholine spin label; SP22A, syringopeptin22A; SP22B, syringopeptin22B; SP25A, syringopeptin25A; SP25B, syringopeptin25B; SPs, syringopeptins; SRE, syringomycin E; SRs, syringomycins; ST, syringotoxin; SUV, small unilamellar vesicles; T_m, main-transition temperature

* Corresponding author. Tel.: +36-1-266-6656; fax: +36-1-266-5666.
E-mail address: grof@puskin.sote.hu (P. Gróf).

0005-2736/$ - see front matter © 2003 Elsevier B.V. All rights reserved.
doi:10.1016/j.bbamem.2003.11.007

lated from bovine seminal plasma and its analogues. Furthermore, a positive charge added to the N-terminus of pardaxin, an icthytoxic peptide, increased the antibacterial activity and enhanced hemolytic activity [18]. Studies on analogues of seminalplasmin and melittin indicated that the hydrophobic momentum of these pore-forming compounds also plays an important role in their activity [4,19].

In this article, another important family of the membrane-permeabilizing compounds, the cyclic lipodepsipeptides (CLPs), is considered. CLPs produced by the phytopathogen *Pseudomonas syringae* pv. *syringae* have also antifungal and antibacterial activity [20–22], which makes them promising compounds to human treatment. CLPs showed different antimicrobal-, hemolytic- and plant pathogenic activity that can be explained by the different structures of these toxins. CLPs have a charged cyclic peptide head and a hydrophobic 3-hydroxy-fatty acid tail of variable length (Fig. 1). There are two groups of the CLPs. The first group includes the nonapeptides: syringomycins (SRs) [12–14], syringotoxin (ST) [23], syringostatins [14] and pseudomycins [24], while the second includes the larger syringopeptins (SPs) [25]. The number of charges and the hydrophobicity of CLPs are variable,

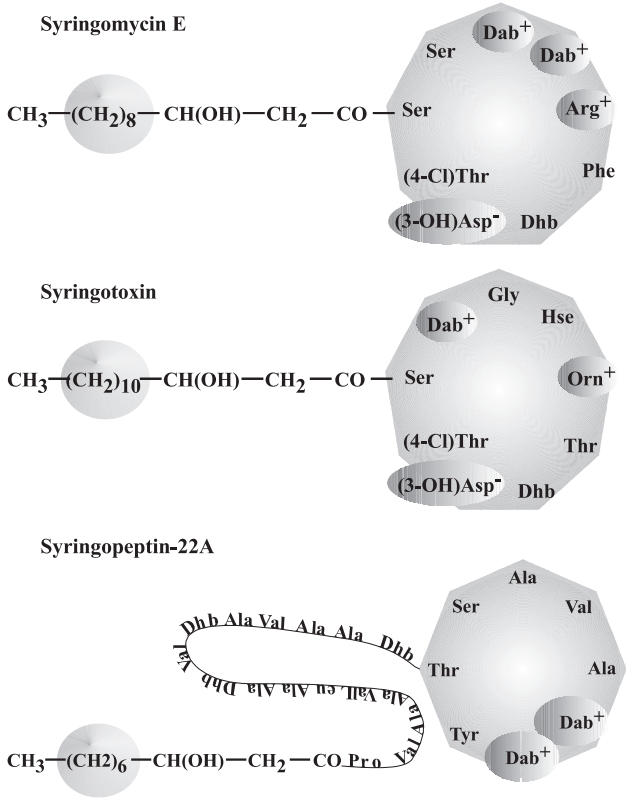

Fig. 1. Schematic structure of the CLPs used in the present study. Abbreviations of the essential amino acids correspond to the generally accepted ones. Abbreviations for the nonessential aminoacids are: Dab: 2,4-diaminobutanoic acid; Dhb: 2,3-dehydro-2-aminobutyric acid; Hse: homoserine; Orn: ornithine.

which suggested having a deterministic role in the activity [26]. The most studied CLP is the nonapeptide syringomycin E (SRE), which possesses a peptide lactone ring with three positive and one negative charges, and a 3-hydroxy-fatty acid tail. The other nonapeptide, ST, studied by us has only two positive charges in addition to one negative on its peptide head, completed with a 3-hydroxy-fatty acid tail. The syringopeptins contain a polar peptide lactone ring built up by eight amino acid residues and has two positive charges. The polar peptide head is joined to the hydrophobic 3-hydroxy-fatty acid tail by a great peptide moiety, which is composed of 14 (SP22A, SP22B) or 17 (SP25A, SP25B) mainly hydrophobic amino acid residues. Thus, the size and the hydrophobicity of SPs are much greater than that of SR or ST. The syringopeptins have stronger phytotoxic activity than the nonapeptides [20,21]. CLPs showed antifungal activity, although different fungal species display different degrees of sensitivity [20,22]. Activity of CLPs is significantly influenced by the lipid composition of the membrane; e.g., the antifungal activities are affected especially by sphingolipids and sterols [27–30]. Lipid involvement in CLP action was also shown with planar bilayer membrane (BLM) and human red blood cells (RBCs) [31–33].

It was shown in earlier studies that SRE, SP22A and ST induce pores on BLM and RBC membrane; SP22A had the highest pore-forming activity, while SRE had less and the weakest was ST [26,34,35]. SRE and ST showed a temperature-dependent pore inactivation. Shorter mean lifetime of the pores was found with ST, than with SRE at 20 and 37 °C. In contrast, SP22A-pores did not inactivate. It was suggested that these differences are the consequences of the variance of hydrophobicity and the number of charges [26].

All the above results highlighted the fact that the structure and the charge both of the pore-forming compounds and the membrane lipids are substantial in the activity. Thus, an investigation of the molecular interactions between the toxins and lipids is essential in order to understand the effect and in favor of rational drug development. Electron paramagnetic resonance (EPR) spectroscopy is a versatile tool to monitor molecular level interactions, which can be different depending on the CLP species and the lipid composition of the model membranes. We focused our study on CLPs acting on liposomes prepared from saturated lipids, DPPC and DMPC. We addressed also the questions: (a) How do CLPs affect the structure of model membranes? (b) How does DOPC, an unsaturated lipid, or cholesterol influence the interactions between the lipids and the CLPs? We monitored the membrane at different depths along the hydrocarbon chain using spin-labeled fatty acids. EPR spectral parameters were used to characterize the membrane fluidity; moreover, rotational dynamics and steric constrains involved in the specific interactions were also determined by simulating the experimental EPR spectra.

2. Materials and methods

2.1. Materials

Cholesterol and synthetic dipalmitoyl-L-α-phoshatidylcholine (DPPC), dimyristoyl-L-α-phoshatidylcholine (DMPC), dioleoyl-phosphatidylcholine (DOPC), of minimum 99% purity, were obtained from Sigma Chemical Co. 7-doxyl (SL-7) and 12-doxyl-stearic acid (SL-12) spin labels were obtained from ICN Biomedicals Inc., Ohio. 16-doxyl-stearic acid (SL-16) spin label was from Sigma Chemical, 5-doxyl-stearic acid (SL-5) spin probe was purchased from Aldrich Chemical Co, 1-palmitoyl-2-stearoyl(5-DOXYL)-*sn*-glycero-3-phosphocholine was obtained from Avanti Polar Lipids INC. SP22A and SRE were purified to homogeneity as described earlier [36] and stored frozen. ST was purified to homogeneity as previously published [36] from cultures of *P. syringae* strain PS268 [37] obtained from D.C. Gross (Texas A & M University, College Station, TX, USA). The CLPs used in our study were a gift from J.Y. Takemoto, Utah State University, USA. Solutions of phosphate buffered saline (PBS) were made from tablets purchased from Oxoid Ltd., Hampshire, England. Ethanol was of analytical grade purchased from Reanal, Hungary.

2.2. Preparation of liposomes

Lipids and the chosen spin label (1 mol%) were dissolved in ethanol. The organic solvent was evaporated with nitrogen stream under continuous rotation of the vessel. The rest of the solvent was removed from the lipid film in 30 min using a vacuum-line and the samples were stored in a desiccator overnight. The dry lipid film was re-hydrated gently above the main transition temperature (at about 50 °C) with PBS (pH: 7.4). To produce multilamellar vesicles (MLV), the dispersion (130 mg lipid/ml) was vortexed for 20 min at 50 °C. To prepare small unilamellar vesicles (SUVs) with different composition, dispersion (10 mg lipid/ml) of the hydrated lipid film was sonicated two times for 10 min, with 10-min pause between sonications, at 50 °C. A Soniprep 150 MSE sonicator was used with frequency of 20 kHz and wave amplitude of 8 μm. The size distribution of the SUV samples was checked by dynamic light scattering (DLS) using an ALV Goniometer. The goniometer was equipped with a Spectraphysics 124B He-Ne laser operating at 10 mW with a wavelength of 632.8 nm. Samples were diluted to the appropriate concentration (~ 1 mg/ml) range for the DLS measurements.

The typical hydrodynamic radius of the vesicles was between 30 and 40 nm with a half-width of about 10 nm.

2.3. Treatment with CLPs

In case of SUVs, 50 μl of liposome dispersion was mixed with an appropriate quantity of toxin (SP22A, SRE or ST) stock solution (1 mg/ml in 10^{-3} M HCl). The CLP/lipid molar ratio used in this study was in the range of 1:40 to 1:800. To check if addition of the CLP's solution does not modify the pH of the final suspension, we added the corresponding volumes of 10^{-3} M HCl solution to PBS and measured the pH. According to this test the highest change in the pH was 0.2. Three protocols were used for the incubation: (a) cold treatment, (b) ambient treatment and (c) warm treatment. *Cold treatment*: before the incubation at 0 °C, all the solutions used were cooled down in ice–water mixture. Liposome dispersion was mixed with the appropiate CLP solution and shaken thoroughly at 5-min incubation time. Aliquots from the sample were put into the EPR tubes maintained also in an ice–water mixture. For the samples prepared at ambient temperature (*ambient treatment*) care has been taken not to exceed 20–23 °C during the CLP treatment before measuring the EPR spectrum. In the *warm treatment*, samples and the CLP solutions were preheated. Samples were treated with the given CLP for 5–10 min at about 37–38 °C in a cell culture thermostat.

In case of MLV, stock solution of the toxin was added to the sample after the rehydration of the lipid film and vortexed for 20 min at ambient temperature to ensure the appropriate mixing of CLPs and lipids.

2.4. ESR spectroscopy

Technical details. EPR spectra were recorded with an X-band Bruker EMX6 on-line spectrometer equipped with a standard rectangular cavity. Modulation frequency was 100 kHz with amplitudes between 0.3 to 2.0 G, depending on the spin label and the sample temperature. For the SL-16 spin label, the maximal amplitude of 0.8 G was chosen below the pretransition temperatures to avoid overmodulation, and it was decreased to 0.3 G at greater temperatures. Similarly, for the other spin labels the modulation amplitudes were greater below the pretransition temperature by 0.5–1.0 G than above the pretransition temperature. Centered at 3400 G, 2048 spectral points were taken in a 100-G interval. Acquisition time was 183 or 366 s with appropriate time constants. The microwave power was 15 mW in the case of SL-5 and SL-7, and 10 mW for the SL-12 and SL-16 spin labels.

Samples were measured in quartz capillaries with inside diameters of about 1.2 mm, centered in the cavity by a special sample holder designed by us. The temperature of the samples was measured and controlled by a fine-wire thermocouple immersed into the sample, and was stabilized with a precision of 0.1 °C with a purpose-built closed circuit, nitrogen-gas system based on Peltier-diodes. Temperature range covered in the present measurements was between 2 and 50 °C.

Evaluation of the EPR spectra. To characterize the membrane fluidity in the case of the spin labels SL-5 and SL-7, we used the parameter $2A_{max}$, the outer-peak separation. In a limited range of temperatures (2–25 °C),

it was possible to determine the value of $2A_{max}$ with satisfying precision also for the SL-12. However, for SL-12 and SL-16, it was necessary to use the ratio of the amplitudes of the low-field peak (h_{+1}) to the center-peak (h_o) (Fig. 2) to characterize the fluidity over the whole temperature range.

To simulate the EPR spectra the latest version of the nonlinear least-squares (NLLS) program developed and

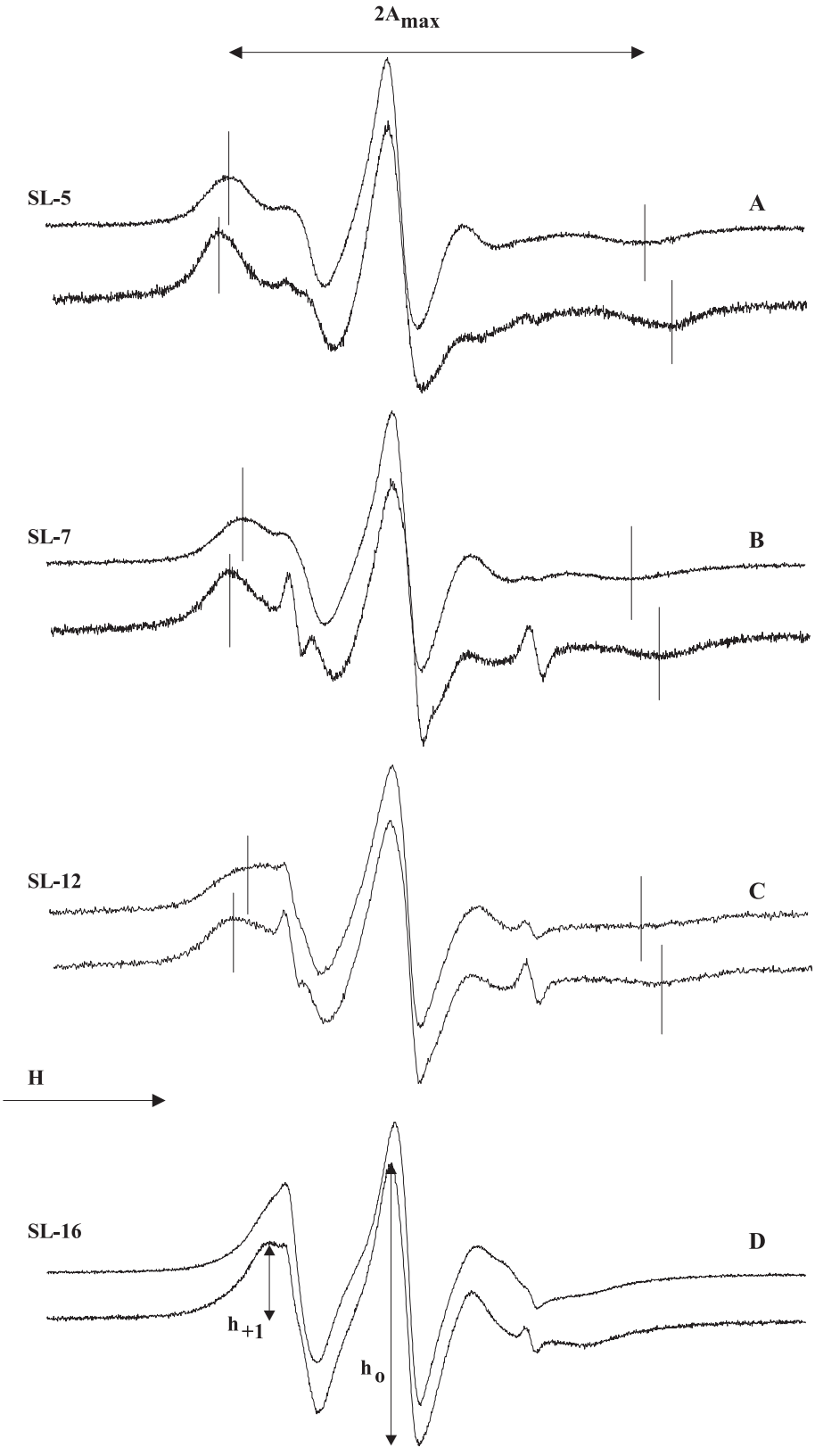

implemented by the Freed's group [38–41] was used. Among other parameters, this program allows determination of the rotational tensor component, R_{prp}, and the ordering potentials, which are connected to the rotational correlation times, and the spatial constrain of the molecular Brownian-motion, respectively. A further quantity is generally derived to characterize the fluidity: the commonly used order parameters, S_{20}, which describes the molecular alignment relative to the main alignment axis. The magnetic parameters used in the calculations were based on earlier experimental and computational results [38,41]. In spectral fitting of the EPR spectra measured with SL-5 spin labels, we used the parameters: $g_{xx}=2.0090$, $g_{yy}=2.0061$, $g_{zz}=2.0026$ and $A_{xx}=6.34$ G, $A_{yy}=5.81$, $A_{zz}=33.1$ G.

3. Results

3.1. Effect of CLPs along the lipid chain

Among the available stearic acid spin labels, four doxyl-stearic acid derivatives are the most frequently used. In these derivatives the doxyl group is attached either to the 5th, 7th, 12th or to the terminal 16th carbon. In an attempt to monitor if there was a region of the lipid chain where the CLPs alter the membrane fluidity, we measured the EPR spectra of these spin labels incorporated into the liposomes. Fig. 2 shows typical EPR spectra of DPPC SUVs labeled by SL-5, SL-7, SL-12 and SL-16 spin labels. In earlier measurements on human RBCs, we found that CLPs produced a remarkable effect on the membrane permeability at a lipid-to-CLP molar ratio of 875–35:1 [26,34,35]. This ratio was 200:1 for the spectra presented in Fig. 2. The molar ratios were calculated taking into account the number of lipid molecules, 3.5×10^{-6} mol, in the outer monolayer of one RBC [42]. Samples were treated according to the ambient protocol for 10 min, heated above the pretransition temperature (about 36 °C) and cooled down to ambient temperature. A remarkable change in the outer-peak separation or in the ratios of h_{+1}/h_o was found with each spin label. The $2A_{max}$ parameters increased by 5, 6 and 5.5 G in case of SL-5, SL-7 and SL-12, respectively (standard deviation: 0.4 G), while the ratio of h_{+1}/h_o in case of SL-16 decreased by 13% (standard deviation: 3%). These observations suggest a substantial decrease of the membrane fluidity along the whole lipid chain. To investigate whether the different inactivation characteristics of the pores obtained on RBCs [26,34,35] were reflected by the fluidity of the structures formed, we measured the EPR spectra of the liposomes treated with SRE using the spin-labeled fatty acids. The molar ratio of the SRE to the lipids was 1:80, which molar ratio we found earlier to be effective on RBCs. The EPR spectra measured (spectra not shown) after same treatment as with SP22A showed an increase of the outer-peak separation, similar to that found with SP22A. With ST a similar effect was found, although the extent of the fluidity change was less, than with SP22A or SRE. Thus, all the three toxins studied by us decreased the fluidity of the lipid bilayer along the whole length of the lipid molecule, which may be an indication of a pore-formation. These observations suggest that the differences in the pore inactivation between SP22A, SRE and ST were not due only to the decreased fluidity. Further differences, especially those in temperature dependence, in the created structures and interactions induced by these toxins should also contribute to the inactivation of the pores.

3.2. Temperature dependence

3.2.1. SUVs

Size distribution of the SUVs was checked by DLS: the mean hydrodynamic radius of the vesicles was about 30 nm with a characteristic S.E. value of 12 nm. Samples were treated on ice with the toxin for less than 10 min according to the cold protocol. In preliminary experiments, we found that even an overnight low-temperature incubation did not change the temperature dependence of the spectra. Temperature was below 10 °C until the start of the measurement. Samples were measured first in heating cycle by increasing the temperature from 2 °C to close to or above the corresponding pretransition temperature (to 33 °C for DPPC and to 20 °C for DMPC). Typical temperature increment was between 2 and 4 °C. No different tendency was observed with greater increments when the temperature remained under about 25 °C for DPPC. SP22A increased the outer-peak separation, which indicates a decrease of membrane fluidity. The temperature dependence of the spectra for DPPC SUV (Fig. 3) showed monotonous decrease of $2A_{max}$ with increasing temperature between 2 and 27 °C. Between 28 and 29 °C there was an abrupt increase in the value of $2A_{max}$; this indicates an abrupt decrease of the fluidity. Above 29 °C the $2A_{max}$ parameter decreased again with increasing temperature indicating the increase of the fluidity. However, the liposome became more rigid in the treated case than in the control one. Samples were then cooled down to 2 °C and the EPR spectra were registered

Fig. 2. EPR spectra of DPPC SUVs: effect of the SP22A on the lipid fluidity. Spin-labeled stearic acid in a maximal concentration of 1 mol% was applied. SL-5, -7, -12 and -16 denote the corresponding stearic acid derivatives, labeled at the 5th, 7th, 12th and 16th carbon atom. Straight lines drawn through the spectra indicate the positions of the outer extrema, where the outer-peak separation, $2A_{max}$, were determined. Also the low-field- and central peak amplitudes, h_{+1} and h_o, are given, which were used in the case of the SL-12 and SL-16 spectra to parameterize the observed changes between the treated and untreated samples. In all cases, the lipid concentration is 10 mg/ml. The SP22A/lipid molar ratio is 1:200. Upper spectrum of each pair corresponds to the untreated liposomes, while the bottom ones were measured on SP22A-treated samples. In the case of SL-12 and SL-16, the measurement temperature was 23 °C, while for SL-7 and SL-5 it was 25 and 27 °C, respectively.

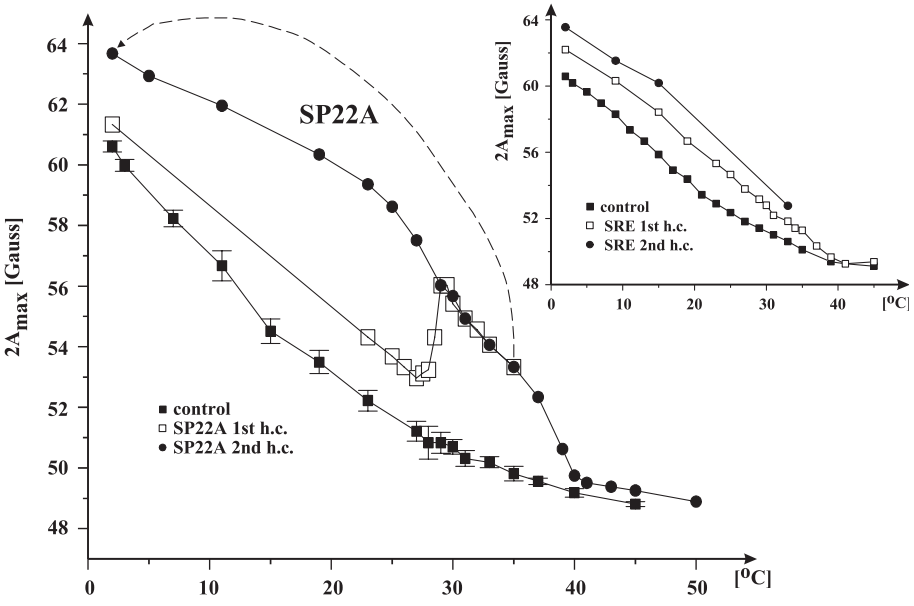

Fig. 3. Effect of the SP22A and the SRE treatments on the temperature dependence of the outer-peak separation after cold treatment. SL-5 spin probe and DPPC SUV were used in both cases. On the main panel, solid squares denote the case control with standard error of mean; open squares correspond to the first heating cycle (h.c.), when the temperature was raised up to 35 °C in case of SP22A-treated samples. The second heating cycle (solid circles) was initiated after cooling down the sample to 2 °C. Inset shows the first heating cycle measured on SUV in case control (solid squares) and on the SRE-treated samples (open squares). The $2A_{max}$ values of the second heating cycle are denoted by solid circles. Toxin-to-lipid molar ratios were 1:200 and 1:80 for the SP22A and the SRE, respectively.

once more in a second heating cycle. A remarkable difference was detected between the outer-peak separations ($2A_{max}$) measured in the two heating cycles with the SL-5 spin probe (Fig. 3). The higher $2A_{max}$ values of the second heating cycle suggested a much smaller fluidity of the lipids in the second cycle than in the first one. The fluidity observed in the two heating cycles coincided, however, beginning from the temperature where the abrupt change in the first heating cycle occurred. In the case of DPPC SUVs, the severe change in fluidity begins at about 27 °C, which is somewhat below the pretransition temperature of DPPC (~ 37 °C). Inspecting the $2A_{max}$ values of the two heating cycles, we found that (a) the increased $2A_{max}$ values measured in the second heating cycle at temperatures lower than 29 °C did not change in subsequent heating or cooling cycles, and (b) above the temperature where the maximal change was found, at about 29 °C, the corresponding values of the second cycle coincide well with those measured in the first heating cycle. These observations suggest that the changes in the fluidity were irreversible.

The inset in Fig. 3 shows the effect of SRE-treatment on the temperature dependence of the outer-peak separations measured on SUV samples with SL-5 spin probe. Both SP22A and SRE considerably decreased the fluidity of the liposomes close to the head regions. The SRE did not initiate severe changes around 29 °C in the dynamics of the lipid head group in the first heating cycle. The corresponding $2A_{max}$ values are 60.61, 61.33 and 61.67 G for the control, SP22A-treated and SRE-treated sample, respectively, in the first heating cycle at 2 °C. When the temperature was increased to 33 °C, we observed the following $2A_{max}$ values: 50.61, 54.39 and 51.83 G for control, SP22A-, and SRE-treated samples, respectively.

In the second heating cycle, however, the SRE-treated DPPC samples showed similar characteristics as we obtained with SP22A, indicating an important change in the structure or organization of the liposomes. It is accompanied by the remarkable change in the $2A_{max}$ values, e.g. at 2 °C, SP22A- and SRE-treated samples showed 63.67 and 63.56 G, respectively, or at 33 °C the maximal hyperfine splitting increased from 51.88 to 52.77 G in SRE-treated samples.

Similar temperature-dependent effect was observed on liposomes prepared from DMPC as on DPPC samples; however, the abrupt fluidity change occurred at lower temperatures. The difference of the $2A_{max}$ parameter between the control and treated samples increased from 1.4 to 2.9 G at 13 °C, and from 2 to 4 G at 19 °C measured on SP22A-, and SRE-treated samples, respectively.

3.2.2. MLVs

The temperature dependence of the EPR spectra obtained with spin-labeled stearic acids for control SUV samples showed quite different behavior from that observed with MLVs. The substantial changes of the outer-peak separation observed for control MLVs around the pretransition were not present in SUV samples even when SL-5 (Fig. 4) or SL-7 (data not shown) were used, which monitor the lipid dynamics close to the polar head group. These temperature dependences indicate the absence of the formation of a

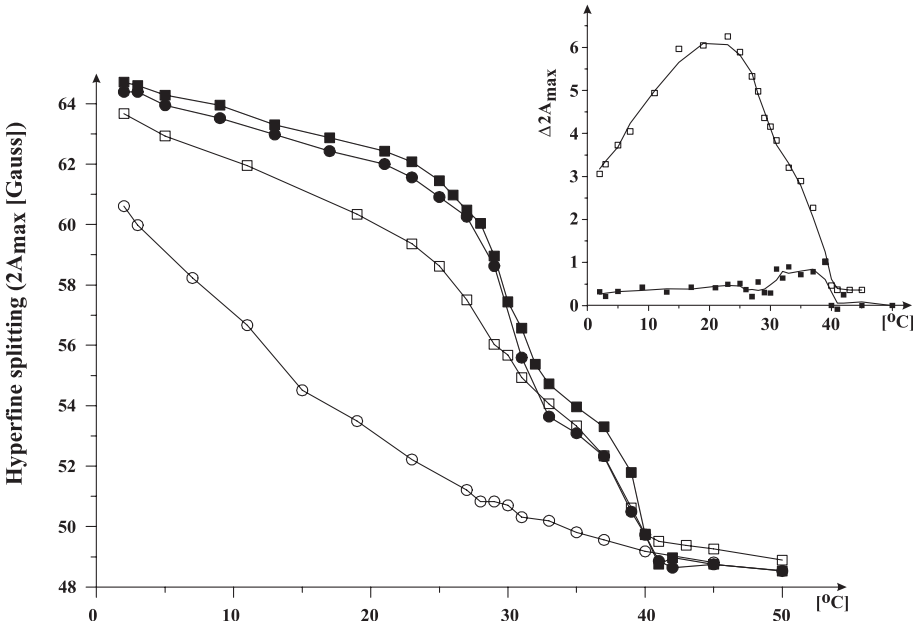

Fig. 4. Effect of SP22A treatment on SUVs and MLVs of DPPC. Main panel: Temperature dependence of the outer-peak separation for SUVs and MLVs. Open circles correspond to case control, and open squares denote syringopeptin-treated samples in the second heating cycle. Closed symbols, circles and squares show the temperature dependence of MLVs for case control and SP22A-treated samples in the first heating cycle, respectively. Inset was generated from the differences in the outer-peak separations, measured for MLV (closed squares) and SUV (open squares) samples, respectively.

ripple structure, which forms if cooperative long-range interaction exists and leads to periodic line defects on the surface of the MLVs or sonicated large unilamellar vesicles (LUVs) [43].

Fig. 4 shows the outer-peak separation for the MLV and SUV DPPC liposomes. Addition of SP22A produces a small but significant decrease in the fluidity of the multibilayer structure below about 29 °C. In case of the SP22A-treated samples the fluidity of both the SUVs and the MLVs decreased above 29 °C up to the main transition as reflected by the increase of $2A_{max}$ relative to the controls. Above the main transition, the fluidity of the two types of liposomes coincides and there was only a small (about 0.4 G) difference in the $2A_{max}$ values of the SP22A-treated samples. The value of $2A_{max}$ changed by more than 7 G at 23 °C in the case of SP22A-treated SUV samples, while the change was smaller (~ 1 G) and shifted to 37 °C for SP22A-treated MLV samples (inset in Fig. 4). These observations suggest a

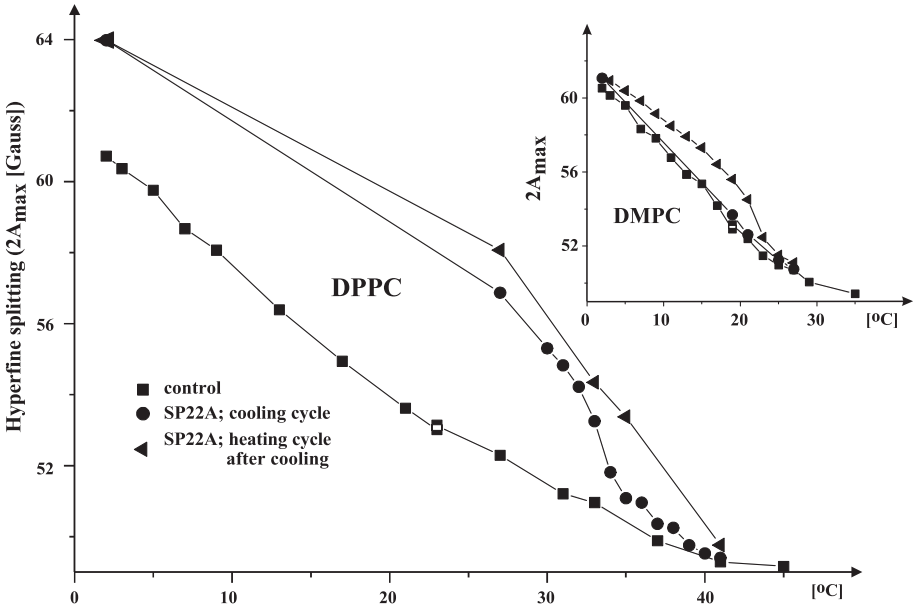

Fig. 5. Temperature dependence of outer-peak separations for SUVs prepared from DPPC and DMPC. Effect of SP22A treatment according to the warm protocol. Symbols given on the main panel are valid also for the inset.

fluidity-modulated impact of the CLPs in the interaction with liposomes, i.e. the change of the fluidity due to the interaction between the CLPs and the liposomes was influenced by the actual fluidity of the liposome itself.

The change of the fluidity observed with increasing temperature, in the direction of the gel-to-fluid transition, could be interpreted as the consequence of temperature dependence of the amount of CLPs, which penetrate into the liposomes' bilayer. At higher temperature, more CLP would penetrate, which would result in a stronger interaction between the CLPs and the lipids. To study this possibility, the temperature dependence of the spectra was also registered in a reversed cycle when the samples were cooled.

3.2.3. Temperature dependence in cooling cycle

Samples were prepared according to the warm protocol (see Materials and methods) and measured in a cooling cycle and in a subsequent heating cycle. Fig. 5 shows typical runs for DPPC- and DMPC SUVs that were treated with SP22A in a molar ratio of 1:200 (SP22A/lipid). The measured $2A_{max}$ values indicated that in the cooling cycle the fluidity of the sample was greater than in the subsequent heating cycle. In case of DPPC, the difference between the fluidities of the cooling cycle and the subsequent heating cycle became smaller, approaching the temperature of the maximal change found in the first cooling cycle (~ 29 °C). To check whether this phenomenon can be attributed to a hysteresis, we prepared DPPC–SP22A samples according to the cold protocol and measured them after the heating cycle in a cooling cycle. In the cooling cycle, we found only a minimal hysteresis, which observation differs from the temperature dependence of the spectra given in Fig. 5.

The inset in Fig. 5 shows similar measurement cycling for DMPC. In the cooling cycle, the measured outer-peak separations ($2A_{max}$) coincide closely with the data measured for the control samples, whereas in the subsequent heating cycle a remarkable difference was observed.

3.3. Effect of cholesterol

Earlier studies on model membranes and on RBCs demonstrated that different sterols modulated the effect of the CLP. Depending on the composition and the species studied, sterols could enhance or diminish the CLPs' effect [9,27,28,31,32,45,46]. In this study SUVs of DPPC–cholesterol were prepared and labeled with the SL-5 spin probe. Fig. 6A shows the results, which correspond to the experimental points measured in the first heating cycle. Three different concentrations of the cholesterol were used: 15, 30 and 40 mol% relative to the host DPPC. To characterize the combined effect of the cholesterol and SP22A, we defined the relative change of the outer-peak separation as $\Delta 2A_{max}/\max(\Delta 2A_{max})$. The term $\Delta 2A_{max}$ denotes the change in the $2A_{max}$ value measured after SP22A treatment of the samples. The other term, $\max(\Delta 2A_{max})$, corresponds to the maximum of the temperature-dependent changes in the

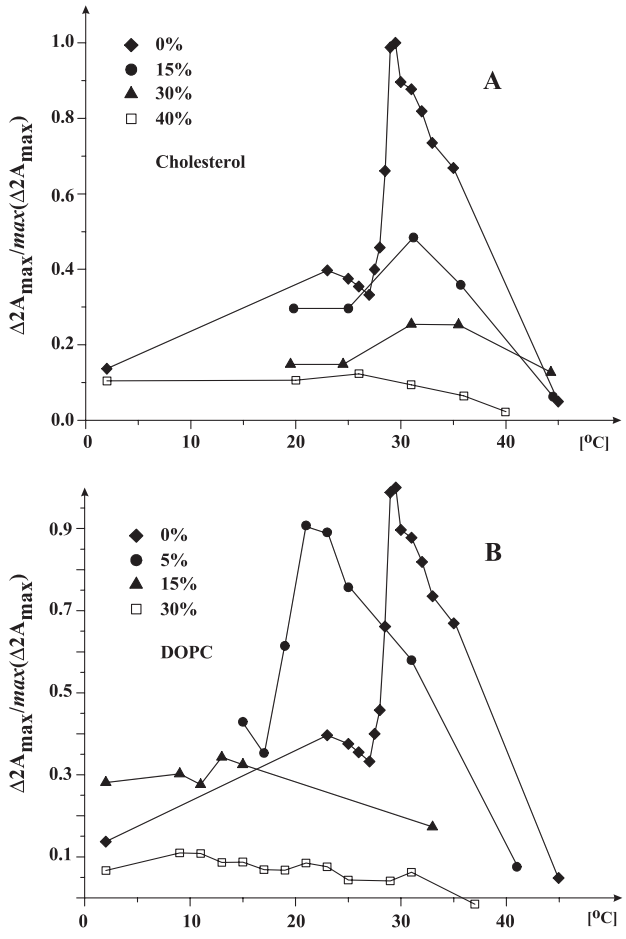

Fig. 6. Dependence of the syringopeptin effect on the lipid composition. Differences in the outer-peak separations between the case control and the first heating cycle of the given sample are normalized for the greatest difference measured in case of syringopeptin-treated DPPC alone. (A) Cholesterol–DPPC SUVs were prepared with 0, 15, 30 and 40 mol% of cholesterol to DPPC. The Cholesterol–DPPC liposomes were treated with a SP22A concentration of 1:200 (SP22A-to-lipid molar ratio) according to the cold protocol. (B) DOPC–DPPC SUVs were prepared with 0, 5, 15 and 30 mol% of DOPC to DPPC. The DOPC–DPPC liposomes were treated in a SP22A-to-lipid molar ratio of 1:200 according to the cold protocol.

$2A_{max}$ values measured for DPPC samples without cholesterol. The defined ratio is 1.0 at the maximum of the change, which occurs at about 29 °C for cholesterol-free sample (Fig. 6A). In the absence of SP22A, the fluidity of the SUV samples decreased relative to the DPPC case control at all cholesterol concentrations, which was reflected by the increased $2A_{max}$ values. The observed decrease depended on the cholesterol concentration: higher concentrations provoked greater decrease in the fluidity. Upon addition of the SP22A, a further decrease was observed in the fluidity (Fig. 6A), but this subsequent change became smaller as the cholesterol content increased.

3.4. Effect of DOPC

In addition to the saturated phospholipids, unsaturated lipids also contribute to the composition of the biological

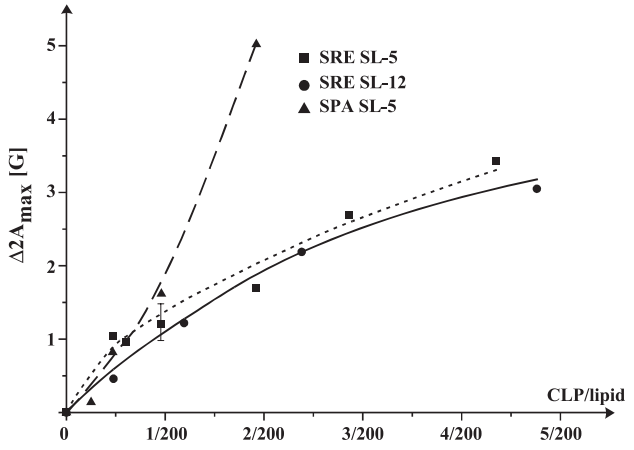

Fig. 7. Change of the maximal hyperfine splitting as the function of the CLP concentration. SUV samples of 10 mg/ml concentration were treated according to the cold protocol and measured in the first heating cycle at 23 °C. $\Delta 2A_{max}$ values denote differences between the case control and the treated sample.

membranes significantly. Among the unsaturated phospholipids, the DOPC is one of the most studied. Therefore, we studied the effect of DOPC on the temperature dependence of the SUV samples treated with SP22A. Fig. 6B shows how the DOPC/DPPC ratio of the liposome composition influences the effect of SP22A in a heating cycle. At 5% DOPC content, there was still severe changes in the fluidity. However, the maximum of the differences between the SP22A-treated and untreated DOPC/DPPC samples shifted to lower temperature (from 29 to 21 °C). The abrupt irreversible change, which was observed with pure DPPC samples, disappeared when the proportion of the DOPC was increased to 15%, indicating that the difference was much smaller between the SP22A-treated and untreated DPPC/DOPC liposomes. In case of the SUVs, which contained 30% DOPC, we observed only little difference between the CLP-treated and untreated samples (Fig. 6B).

3.5. Concentration dependence of fluidity change in SP22A- and SRE-treated liposomes

Concentration dependence of the CLP-lipid interaction was studied at 23 °C (Fig. 7), below the temperature of the rigidity step, which occurs for DPPC SUV samples at about 29 °C (see Fig. 3). Our argument to observe the concentration dependence below this temperature is that: (a) the temperature of the irreversible fluidity step varies depending on the toxin; (b) at 29 °C even a SP22A/lipid ratio of 1:200 provoked a great change in the outer-peak separation. Fig. 7 shows that for both SP22A and SRE, the effect of CLP is detectable at least at a CLP/lipid ratio of 1:400. We were also able to detect similar decrease of the fluidity at the middle of the hydrocarbon chain with the SL-12 spin probe. It is detectable even for the SRE, which according to our measurements induces smaller change than the SP22A at the same concentration.

4. Discussion

4.1. Pore-formation by CLPs of P. syringae pv. syringae

According to earlier measurements, the CLPs form pores on RBC- and model membranes [7,9,33–35,47–49]. In agreement with our experimental observations, our spectral simulation revealed an increased ordering and hindered rotation of the lipid molecules when they interacted with CLPs. Table 1 contains some indicative data for the calculated order parameters and rotational correlation times. The phenomenon that CLPs increased the order along the whole lipid-chain corresponds to the observations [6,8–10] that CLPs induce pores. Based on single-channel measurements a recent hypothesis proposed [33] that the pores formed by the SRE were built up from a lipid core stabilized by the toxin molecules. On the bases of simple geometrical model, it has also been proposed that the number of lipid molecules involved in a pore created by one SRE monomer was roughly 40. In the present work, CLP/lipid molar ratios between about 1:40 (2.5 mol%) and 1:800 (0.125 mol%) were investigated with SP22A and SRE. In the case of SP22A and SRE, the EPR spectra have shown a significant change in the fluidity, beginning from the CLP/lipid ratio ~ 1:400. Inspection of the spectra measured for these cases showed no sign of two lipid populations, which would belong to bulk and "pore" lipids. In accordance with the experimental spectra, also our spectral simulations proved no sign of a two-component spectrum in case of any spin label. Lack of observing two component spectra in gel phase membranes, however, does not necessarily mean involvement of the majority of the lipids in pore-formation. Ability to detect two components of different mobility is determined by at least two factors: (a) exchange rate between "bound" and bulk lipids; (b) the difference in the correlation times/ordering potential of the two compartments [50]. Time scale of the molecular motions in gel phase membranes corresponds rather to the time scale of the ST-EPR spectroscopy [51,52]. Thus, experimental determination of the bulk/bound ratio would require detailed ST-EPR measurements, which, however, is beyond the scope of the present work.

Lipid–protein interaction was studied mainly on proteins of much greater molecular weight then the CLPs, e.g. avidin

Table 1
Best-fit parameters of R_{prp} and S_{20} from NLLS fits for ESR spectra of DPPC liposomes labeled with SL-5

	Control	First heating cycle	Second heating cycle
S_{20}[a]	0.49	0.52	0.67
R_{prp} [s^{-1}][b]	5.56×10^7	4.57×10^7	3.47×10^7

Values given in the table were determined with EPR spectral simulations. The fitted experimental spectra were measured at 27 °C. DPPC samples were treated with syringpopeptin 22A in a toxin-to-lipid ratio of 1:200.

[a] Value of the S.E. is ± 0.01.

[b] Range of the S.E. is ± 5% for the determination of the rotational correlation time.

possesses a molecular weight of 66 kDa [53], while the greatest CLP in our study, SP22A, has that of 2200. This difference in molecular dimension can suggest that the primary shell of lipids, nearest to the CLPs, can build up a highly ordered domain that, together with the toxin, exerts aligning potential for the subsequent shells of lipid molecules. In case of SUVs, this event can lead to a continuous change of the molecular ordering and the rotational correlation time of the lipids along the shells. The observed EPR spectrum is then the average of a great number of highly or moderately ordered lipid molecules, for which the estimated number of 40 may be the minimal estimate. This explanation may also suggest that pores formed by CLPs may be built up from varying number of lipid molecules. The number of lipid molecules involved in one pore can depend on the lipid composition of the membrane.

We were also faced to the question if there is a specific interaction between the spin-labeled stearic acid derivatives and the CLPs, which can lead to preferential or specific involvement of the spin label molecules in pore formation, hence selective interaction of different lipids are well documented in the works of Marsh's group [53]. Thus, the EPR spectra were not representative of the whole membrane but only to the specific interaction between the toxin and spin labels. A verification for the exclusion of the above possible specific interaction is the use of, e.g. spin-labeled phosphatidyl-choline. In a control experiment with SL-SPPC using SP22A in a CLP/lipid ratio of 1:100, we observed similar change in the membrane fluidity as with the spin-labeled stearic acid derivative. Although this simple test gives evidence that CLPs have an effect on DPPC below the main transition, it does not completely exclude that the large effect observed using SL spin labels is the result of the combined effects on the host lipid and the specific interaction between CLPs and SL spin probes.

4.2. Heating vs. cooling cycle

The DPPC and DMPC samples prepared according to the cold protocol and measured in the first heating cycle showed an abrupt irreversible decrease of the fluidity at a temperature characteristic for the lipid species. This phenomenon could have been attributed to temperature-dependent changes in the incorporation depth of the CLPs. In this case, the SP22A-treated samples, prepared according to the warm protocol, should have shown high $2A_{max}$ values due to the great amount of SP22A that entered into the membrane. Inconsistent with this hypothesis, the $2A_{max}$ values, measured in the cooling cycle (Fig. 6) above the main transition temperature of the DPPC or DMPC, were close to the control values. Significant differences in the $2A_{max}$ values between the control and the treated samples were detected only close to the pretransition temperature in case of the DPPC. Accordingly, the abrupt change of the fluidity cannot be explained by the change in the incorporation depth. It seems that the change in the fluidity occurs close to the pretransition within a relatively narrow temperature range. EPR spectra of the SRE-treated samples measured in heating cycle after cold treatment showed similar irreversible change as the samples treated with SP22A, although the required temperature was higher (36 °C) than with SP22A. These suggest that specific molecular interaction presumably between both the head groups and the hydrocarbon chains are required for the abrupt fluidity change. The hydrophobicity of the SRE is smaller than that of SP22A, which can be responsible for difference between the transition temperatures, and it can explain that the SP22A may exert the strongest impact on the ordering and mobility of the lipid molecules among the three toxins. Temperature dependence of effect on the fluidity of the three toxins, together with the concentration dependence of their ordering activity, may provide a reasonable explanation for the differences of the pore inactivation. Inactivation can be thought as disruption of the pores due to the lower alignment and greater motional freedom of the lipid molecules in the case of SRE and ST than for SP22A.

4.3. Influence of cholesterol and DOPC in CLP action

Among other techniques DSC, X-ray and spectroscopic measurements have shown that cholesterol increases the hydration of the headgroups, increases the acyl chain ordering and reduces the water penetration [54–59]. Studying calcein efflux from LUVs using syringopeptins, syringomycin-E and ST, the minimal CLP-to-lipid ratio was 1:10 in the work of Dalla Serra et al. [9]. The effect of SP22A was found maximal even without sterols, but SRE and ST have shown an increase in their activity if specific sterols were used preparing the LUV. According to our present results, the cholesterol (Chol) was not necessary to induce a remarkable change in the fluidity of the SUV interacting with CLPs. Instead, the largest relative decrease in the fluidity was found without adding cholesterol.

In our measurements (data not shown here), we observed that Chol decreased the membrane fluidity proportional to its increasing concentration in DPPC–Chol SUV samples. What may be the origin of the results that with increasing Chol content we observed a decreasing extent in the CLP rigidifying effect? A possible explanation is that there is an upper limit for the ordering and reduced mobility of the lipid molecules at a given temperature. This corresponds to the case of the MLV, where the lipid ordering is the highest one due to the inter- and intrabilayer forces. Indeed, in the case of MLV compared to SUV we observed a smaller apparent decrease of the fluidity, induced by SP22A (Fig. 4).

It seems, therefore, that the presence of the cholesterol/sterols is not a prerequisite for the CLP action, at least not in its action to build up ordered shells from lipid molecules of increased ordering. The lower effect of SP22A on cholesterol-containing SUVs is in agreement with the study [32], which showed that on cholesterol-depleted RBCs the pore-forming activity of SRE was higher than on control RBCs.

Furthermore, it was shown that the rate of increase for bilayer conductance induced by SRE was about 1000 times less in bilayers containing 50 mol% of cholesterol than in bilayers without sterols [31].

Biological membranes contain significant amount of unsaturated lipids, from which the most studied is the DOPC. Its main transition temperature is about −22 °C [60]. The hydrocarbon chain of DOPC possesses greater motional freedom than that of DPPC due to the unsaturated bond in DOPC [61]. Permeability measurements on RBCs and on BLMs—prepared from DOPS/DOPE binary mixtures—proved, however, that pores exist also in that case and the pore's lifetime decreases with increasing fluidity [7,8,26,32–35]. Our results show that as far as the temperature was increased close to the main transition temperature, which corresponds to an increased fluidity, the difference between the treated and untreated DPPC samples diminished. Thus, the greater motional freedom can decrease the ability of the CLPs to order the lipids in the DOPC–DPPC mixtures to the extent observed with DPPC alone. This explains that although the pores can exist at relatively high thermal fluctuation, the difference between the EPR spectra of the ordered and disordered lipids becomes very small, which leads to almost no difference between the EPR spectra of the treated and the untreated samples.

4.4. Coalescence, aggregation

Our data suggested that the fluctuations in the highly curved SUVs did not allow the ordering of the chain melting-induced point defects into line defects that were necessary for the pretransition [43,44]. In the case of SUVs, there is no bilayer–bilayer interaction; the out-of-plane fluctuations are less confined than in the case of MLVs or LUVs, and only those curvature fluctuations are allowed, which maintain the closed topology [43].

Temperature dependence of the fluidity of the SP22A-treated DPPC SUV samples in the second heating cycle was very close to that one observed with MLVs (Fig. 4). These results suggest the appearance of such new structures in the interaction with CLPs, which make possible the inter-bilayer interactions, and stronger surface confinements and can result in: (a) increase of the vesicle radius; (b) induce aggregation. Both cases can lead to formation of the ripple structure in the treated samples, thereby approaching the temperature dependence observed for a more ordered and confined liposome system, the MLV. Indeed, in the case when we detected the abrupt irreversible change of the fluidity, careful check of the CLP-treated samples showed increased turbidity and aggregation of the vesicles. An increase of the vesicle radius can be resulted in either by fusion or coalescence of the unilamellar vesicles. Our preliminary DLS and EPR measurements showed that apart from aggregation, coalescence of the SUVs occurred at temperatures somewhat below the pretransition when SP22A, SRE or ST interacts with SUVs (data are not shown). These observations do not exclude the possibility of vesicle fusion.

5. Conclusion

Our experimental works and computer simulations have shown that pore formation caused by SP22A, SRE and ST likely involves lipid molecules aligning them in ordered, motionally constrained structure. The number of lipid molecules involved in a pore may vary depending on the CLP species, concentration, and the lipid composition of the membrane. Comparing MLVs and SUVs, we observed that the ability of the CLPs to order the lipid molecules involved in pore formation depends also on the motional freedom of the lipid molecules constrained by the specific interactions acting in the liposomal structures. The highest activity to modify lipid ordering was found for SP22A, while SRE was less active and ST the least one. Cholesterol increased, while DOPC decreased the ordering of the lipid molecules in SUVs and both limited the additional ordering effect of the SP22A on the lipid molecules. Comparing EPR spectra measured in heating and cooling cycles for DPPC and DMPC samples, we have shown that the abrupt change in the fluidity measured on CLP-treated SUVs occurred within a limited range of temperatures. This fluidity change is due to coalescence and aggregation of the SUVs, which can have importance in bacterial attack. Further efforts are required to understand the effect of different sterols and the phenomenon of fusion/coalescence.

Acknowledgements

We thank J.Y. Takemoto for supplies of the purified cyclic lipodepsipeptides. The authors gratefully thank Dr. Módos for the technical help and for the evaluation of the DLS measurements, and Mrs. É. Bányay for the skilled technical assistance. This research was supported by grants from the Hungarian Ministry of Health (ETT 486/96; ETT 229/2000).

References

[1] G. Saberwal, R. Nagaraj, Cell-lytic and antibacterial peptides that act by perturbing the barrier function of membranes: facets of their conformational features, structure–function correlations and membrane-perturbing abilities, Biochim. Biophys. Acta 1197 (1994) 109–131.
[2] W.L. Maloy, U.P. Kari, Structure–activity studies on magainins and other host defense peptides, Biopolymers (Pept. Sci) 37 (1995) 105–122.
[3] K. Matsuzaki, Magainins as paradigm for the mode of action of pore forming polypeptides, Biochim. Biophys. Acta 1376 (1998) 391–400.
[4] N. Sitaram, R. Nagaraj, Interaction of antimicrobial peptides with biological and model membranes: structural and charge requirements for activity, Biochim. Biophys. Acta 1462 (1999) 29–54.

[5] R.J. Gilbert, Pore-forming toxins, Cell. Mol. Life Sci. 59 (5) (2002) 832–844.
[6] M.L. Hutchinson, M.A. Tester, D.C. Gross, Role of biosurfactant and ion channel-forming activities of syringomycin in transmembrane ion flux: a model for the mechanism of action in the plant–pathogen interaction, Mol. Plant-Microb. Interact. 8 (4) (1995) 610–620.
[7] A.M. Feigin, J.Y. Takemoto, R. Wangspa, J.H. Teeter, J.G. Brand, Properties of voltage-gated ion channels formed by syringomycin E in planar lipid bilayers, Membr. Biol. 149 (1996) 41–47.
[8] M.L. Hutchinson, D.C. Gross, Lipopeptide phytotoxins produced by *Pseudomonas syringae* pv. *syringae*: comparison of the biosurfactant and ion channel-forming activities of syringopeptin and syringomycin, Mol. Plant-Microb. Interact. 10 (3) (1997) 347–354.
[9] M. Dalla Serra, G. Fagiuoli, P. Nordera, I. Bernhart, C. Della Volpe, D. Di Giorgio, A. Ballio, G. Menestrina, The interaction of lipodepsipeptide toxins from *Pseudomonas syringae* pv. *syringae* with biological and model membranes: a comparison of syringotoxin, syringomycin, and two syringopeptins, Mol. Plant-Microb. Interact. 12 (5) (1999) 391–400.
[10] M. Dalla Serra, I. Bernhart, P. Nordera, D. Di Giorgio, A. Ballio, G. Menestrina, Conductive properties and gating of channels formed by syringopeptin 25A, a bioactive lipodepsipeptide from *Pseudomonas syringae* pv. *syringae*, in planar lipid membranes, Mol. Plant-Microb. Interact. 12 (5) (1999) 401–409.
[11] G. Menestrina, M.D. Serra, G. Prevost, Mode of action of beta-barrel pore-forming toxins of the staphylococcal alpha-hemolysin family, Toxicon 39 (11) (2001) 1661–1672.
[12] A. Segre, R.C. Bachmann, A. Ballio, F. Bossa, I. Grgurina, N.S. Iacobellis, G. Marino, P. Pucci, M. Simacco, J.Y. Takemoto, The structure of syringomycins A1, E and G, FEBS Lett. 255 (1989) 27–31.
[13] E. Vaillo, A. Ballio, P.-L. Luisi, R.M. Thomas, The spectroscopic properties of the lipodepsipeptide, syringomycin E, Biopolymers 32 (1992) 1317–1326.
[14] N. Fukuchi, A. Isogai, J. Nakayma, S. Takayama, S. Yamasita, K. Suyama, J.Y. Takemoto, A. Suzuki, Structure and stereochemistry of three phytotoxins, syringomycin, syringotoxin and syringostatin, produced by *Pseudomonas syringae* pv. *syringae*, J. Chem. Soc., Perkin Trans. 1 (1992) 1149–1157.
[15] A. Ballio, F. Bossa, D. Di Giorgio, A. Di Nola, C. Manetti, M. Paci, A. Scaloni, A.L. Segre, Solution conformation of the *Pseudomonas syringae* pv. *syringae* phytotoxic lipodepsipeptide syringopeptin 25-A. Two-dimensional NMR, distance geometry and molecular dynamics, Eur. J. Biochem. 234 (1995) 747–758.
[16] N. Sitaram, C. Subbalakshmi, R. Nagaraj, Structural and charge requirements for antimicrobial and hemolytic activity in the peptide PKLLETFLSKWIG, corresponding to the hydrophobic region of the antimicrobial protein bovine seminalplasmin, Int. J. Pept. Protein Res. 46 (1995) 166–173.
[17] N. Sitaram, M. Chandy, V.N.R. Pillai, R. Nagaraj, Change of glutamic acid to lysine in a 13-residue antibacterial and hemolytic peptide results in enhanced antibacterial activity without increase in hemolytic activity, Antimicrob. Agents Chemoter. 36 (1992) 2468–2472.
[18] Z. Oren, Y. Shai, A class of highly potent antibacterial peptides derived from pardaxin, a pore-forming peptide isolated from Moses sole fish *Pardachirus marmoratus*, Eur. J. Biochem. 237 (1) (1996) 303–310.
[19] E. Perez-Paya, R.A. Houghten, S.E. Blondelle, The role of amphipathicity in the folding, self-association and biological activity of multiple subunit small proteins, J. Biol. Chem. 270 (3) (1995) 1048–1056.
[20] P. Lavermicocca, N. Sante Iacobellis, M. Simmaco, A. Graniti, Biological properties and spectrum of activity of *Pseudomonas syringae* pv. *syringae* toxins, Physiol. Mol. Plant Pathol. 50 (1997) 129–140.
[21] D. Di Giorgio, L. Camoni, K.A. Mott, J.Y. Takemoto, A. Ballio, Syringopeptins, *Pseudomonas syringae* pv. *syringae* phytotoxins, resemble syringomycin in closing stomata, Plant Pathol. 45 (1996) 564–571.
[22] K.N. Sorensen, K.H. Kim, J.Y. Takemoto, In vitro antifungal and fungicidal activities and erythrocyte toxicities of cyclic lipodepsinonapeptides produced by *Pseudomonas syringae* pv. *syringae*, Antimicrob. Agents Chemother. 40 (1996) 2710–2713.
[23] A. Ballio, F. Bossa, A. Collina, M. Gallo, N.S. Iacobellis, M. Paci, P. Pucci, A. Scaloni, A. Segre, M. Simacco, Structure of syringotoxin, a bioactive metabolite of *Pseudomonas syringae* pv. *syringae*, FEBS Lett. 269 (2) (1990) 377–380.
[24] A. Ballio, F. Bossa, D. Di Giorgio, P. Ferranti, M. Paci, P. Pucci, A. Scaloni, G.A. Segre, Novel bioactive lipodepsipeptides from *Pseudomonas syringae*: the pseudomycins, FEBS Lett. 355 (1) (1994) 96–100.
[25] A. Ballio, D. Barra, F. Bossa, A. Collina, I. Grgurina, G. Marino, G. Moneti, M. Paci, P. Pucci, A. Segre, M. Simmaco, Syringopeptins, new phytotoxic lipodepsipeptides of *Pseudomonas syringae* pv. *syringae*, FEBS Lett. 291 (1991) 109–112.
[26] Zs. Szabo, P. Grof, L.V. Schagina, P.A. Gurnev, J.Y. Takemoto, E. Matyus, K. Blasko, Syringotoxin pore formation and inactivation in human red blood cell and model bilayer lipid membranes, BBA 1567 (1–2) (2002) 143–149.
[27] R. Wangspa, J.Y. Takemoto, Role of ergosterol in growth inhibition of *Saccharomyces cerevisiae* by Syringomycin E, FEMS Microbiol. Lett. 167 (1998) 215–220.
[28] C. Julmanop, Y. Takano, J.Y. Takemoto, T. Miyakawa, Protection by sterols against the cytotoxicity of syringomycin in the yeast *Saccharomyces cerevisiae*, J. Gen. Microbiol. 139 (1993) 2323–2327.
[29] H. Hama, D.A. Young, J.A. Radding, D. Ma, J. Tang, S.D. Stock, J.Y. Takemoto, Requirement of sphingolipid α-hydroxylation for fungicidal action of syringomycin E, FEBS Lett. 478 (1–2) (2000) 26–28.
[30] S.D. Stock, H. Hama, J.A. Radding, D.A. Young, J.Y. Takemoto, Syringomycin E inhibition of *Saccharomyces cerevisiae*: requirement for biosynthesis of sphingolipids with very-long-chain fatty acids and mannose- and phosphoinositol-containing head groups, Antimicrob. Agents Chemoter. 44 (5) (2000) 1174–1180.
[31] A.M. Feigin, L.V. Schagina, J.Y. Takemoto, J.H. Teeter, J.G. Brand, The effect of sterols on the sensitivity of membranes to the channel-forming antifungal antibiotic, syringomycin E, Biochim. Biophys. Acta 1324 (1997) 102–110.
[32] K. Blasko, L.V. Schagina, G. Agner, Yu.A. Kaulin, J.Y. Takemoto, Membrane sterol composition modulates the pore forming activity of syringomycin E in human red blood cells, Biochim. Biophys. Acta 1373 (1998) 163–169.
[33] V.V. Malev, L.V. Schagina, P.A. Gurnev, J.Y. Takemoto, E.M. Nestorovich, S.M. Bezrukov, Syringomycin E channel: a lipidic pore stabilized by lipopeptide? Biophys. J. 82 (4) (2002) 1985–1994.
[34] G. Agner, Y.A. Kaulin, L.V. Schagina, J.Y. Takemoto, K. Blasko, Effect of temperature on the formation and inactivation of syringomycin E pores in human red blood cells and bimolecular lipid membranes, Biochim. Biophys. Acta 1466 (1–2) (2000) 79–86.
[35] G. Agner, Y.A. Kaulin, P.A. Gurnev, Z. Szabo, L.V. Schagina, J.Y. Takemoto, K. Blasko, Membrane-permeabilizing activities of cyclic lipodepsipeptides, syringopeptin 22A and syringomycin E from *Pseudomonas syringae* pv. *syringae* in human red blood cells and in bilayer lipid membranes, Bioelectrochemistry 52 (2) (2000) 161–167.
[36] A.P. Bidwai, L. Zhang, R.C. Bachmann, J.Y. Takemoto, Mechanism of action of *Pseudomonas syringae* phytotoxin syringomycin. Stimulation of red beef plasma membrane ATPase activity, Plant Physiol. 83 (1987) 39–43.
[37] D.C. Gross, J.E. De Vay, F.H. Stadtman, Chemical properties of syringomycin and syringotoxin: toxigenic peptides produced by *Pseudomonas syringae*, J. Appl. Bacteriol. 43 (1977) 453–463.
[38] E. Meirovitch, A. Nayeem, J.H. Freed, Analysis of protein–lipid interactions based on model simulations of electron spin resonance spectra, J. Phys. Chem. 88 (1984) 3454–3465.
[39] E. Meirovitch, D. Igner, E. Igner, G. Moro, J.H. Freed, Electron-spin relaxation and ordering in smectic and supercooled nematic liquid crystals, J. Chem. Phys. 77 (1982) 3915–3938.

[40] M. Ge, D.E. Budil, J.H. Freed, ESR studies of spin-labeled membranes aligned by isopotential spin-dry ultracentrifugation: lipid–protein interactions, Biophys. J. 67 (1994) 2326–2344.
[41] D.E. Budil, S. Lee, S. Saxena, J.H. Freed, Nonlinear-least-squares analysis of slow-motion EPR spectra in one and two dimensions using a modified Levenberg–Marquardt algorithm, J. Magn. Res. 120 (1996) 139–284.
[42] S.R. Hollan, J.H. Breuer, J.G. Szelényi, On the red cell membrane, Haematologia 6 (1972) 221–236.
[43] T. Heimburg, A model for the lipid pretransition: coupling of ripple formation with the chain-melting transition, Biophys. J. 78 (2000) 1154–1165.
[44] M.F. Schneider, D. Marsh, W. Jahn, B. Kloesgen, T. Heimburg, Network formation of lipid membranes: triggering structural transitions by chain melting, Proc. Natl. Acad. Sci. U. S. A. 96 (1999) 14312–14317.
[45] N. Taguchi, Y. Takano, C. Julmanop, Y. Wang, S. Stock, J. Takemoto, T. Miyakawa, Identification and analysis of the *Saccharomyces cerevisiae* SYR1 gene reveals that ergosterol is involved in the action of syringomycin, Microbiology 140 (1994) 353–359.
[46] J.Y. Takemoto, Y. Yu, S.D. Stock, T. Miyakawa, Yeast genes involved in growth inhibition by *Pseudomonas syringae* pv. *syringae* syringomycin family lipodepsipeptides, FEMS Microbiol. Lett. 114 (1993) 339–342.
[47] L.V. Schagina, Y.A. Kaulin, A.M. Feigin, J.Y. Takemoto, J.G. Brand, V.V. Malev, Properties of ionic channels formed by the antibiotic syringomycin E in lipid bilayers: dependence on the electrolyte concentration in the bathing solution, Membr. Cell Biol. 12 (1998) 537–555.
[48] Y.A. Kaulin, L.V. Schagina, S.M. Bezrukov, V.V. Malev, A.M. Feigin, J.Y. Takemoto, J.H. Teeter, J.G. Brand, Cluster organization of ion channels formed by the antibiotic syringomycin E in bilayer lipid membranes, Biophys. J. 74 (1998) 2918–2925.
[49] V.V. Malev, Y.A. Kaulin, S.M. Bezrukov, P.A. Gurnev, J.Y. Takemoto, L.V. Shchagina, Kinetics of opening and closure of syringomycin E channels formed in lipid bilayers, Membr. Cell Biol. 14 (2001) 813–829.
[50] D. Marsh, L.I. Horváth, Structure, dynamics and composition of the lipid–protein interface. Perspectives from spin-labelling, Biochim. Biophys. Acta 1376 (3) (1998) 267–296.
[51] A. Watts, D. Marsh, Saturation transfer ESR studies of molecular motion in phosphatidylglycerol bilayers in the gel phase, Biochim. Biophys. Acta 642 (1981) 231–241.
[52] L.I. Horvath, P.J. Brophy, D. Marsh, Spin label saturation transfer EPR determinations of the stoichiometry and selectivity of lipid–protein interactions in the gel phase, Biochim. Biophys. Acta 1147 (2) (1993) 277–280.
[53] M.J. Swamy, D. Marsh, Spin-label electron paramagnetic resonance studies on the interaction of avidin with dimyristoyl-phosphatidylglycerol membranes, Biochim. Biophys. Acta 1513 (2001) 122–130.
[54] P.L. Yeagle, Cholesterol and the cell membrane, Biochim. Biophys. Acta 822 (1985) 267–287.
[55] B.D. Ladbrooke, R.M. Williams, D. Chapman, Studies on lecithin–cholesterol–water interaction by differential scanning calorymetry and X-ray diffraction, Biochim. Biophys. Acta 150 (1968) 333–340.
[56] M. Ge, J.H. Freed, Electron-spin resonance study of aggregation of gramicidin in dipalmitoylphosphatidylcholine bilayers and hydrophobic mismatch, Biophys. J. 76 (1999) 264–280.
[57] S.A. Simon, T.J. McIntosh, R. Latorre, Influence of cholesterol on water penetration into bilayers, Science 216 (1982) 65–67.
[58] T.P. McMullen, C. Vilcheze, R.N. McElhaney, R. Bittman, Differential scanning calorimetric study of the effect of sterol side chain length and structure on dipalmitoylphosphatidylcholine thermotropic phase behavior, Biophys. J. 69 (1995) 169–176.
[59] T.P. McMullen, R.N. Lewis, R.N. McElhaney, Differential scanning calorimetric and Fourier transform infrared spectroscopic studies of the effects of cholesterol on the thermotropic phase behavior and organization of a homologous series of linear saturated phosphatidylserine bilayer membranes, Biophys. J. 79 (2000) 2056–2065.
[60] S. Kaneshina, H. Ichimori, T. Hata, H. Matsuki, Barotropic phase transitions of dioleoylphosphatidylcholine and stearoyl-oleoylphosphatidylcholine bilayer membranes, Biochim. Biophys. Acta 1374 (1998) 1–8.
[61] C.D. Stubbs, T. Kouyama, K. Kinosita Jr., A. Ikegami, Effect of double bonds on the dynamic properties of the hydrocarbon region of lecithin bilayers, Biochemistry 20 (1981) 4257–4262.